SEISMIC RESPONSE OF A PC CABLE-STAYED BRIDGE SUBJECTED TO A LONG-PERIOD GROUND MOTION

G. Shoji[1], T. Kogi[2] and Y. Umesaka[2]

[1] *Associate Professor, Dept. of Engineering Mechanics and Energy , University of Tsukuba, Tsukuba, Japan*
[2] *Former Undergraduate Student, College of Engineering Systems, University of Tsukuba, Tsukuba, Japan*
Email: gshoji@kz.tsukuba.ac.jp

ABSTRACT :
In this study, the mechanisms associated with the seismic response of a long-period bridge when subjected to a long-period ground motion are clarified. First, a typical cable-stayed bridge with prestressed concrete girders (PC cable-stayed bridge) was selected for analysis and modeled for shaking table tests in consideration of the similarity law. Second, shaking table tests of the PC cable-stayed bridge model were carried out to clarify the mechanisms involved, focusing on the linear and nonlinear seismic behaviors of the tower and cables by using the long-period components of the simulated ground motions in the 1999 Chi-Chi, Taiwan earthquake and the simulated long-period ground motions in the anticipated Nankai earthquake as the input ground motions.

KEYWORDS:
long-period ground motion, long-period bridge, PC cable-stayed bridge, seismic response, shaking table test

1. INTRODUCTION

In recent years, the damage to infrastructure caused by a long-period and long-duration ground motion induced by a far-field earthquake has been concerned more extensively. One of the reason for this is that large far-field earthquakes have occurred such as the 2003 Tokachi-oki earthquake and the 2004 Sumatra-Andaman earthquake. In addition to these earthquakes, the seismic risks induced by a Tokai, Toh-Nankai, and Nankai earthquakes in the next 30 years, which are typical far-field earthquakes, are considered to be very high in Japan. Many researchers are involved in computer-based simulations to predict long-period ground motions due to a large far-field earthquake. Kamae *et al.*(2004) carried out a simulation of the ground motions that would be excited in the Osaka Plains due to the anticipated Nankai earthquake using the finite differential method. Otsuka *et al.*(1998) evaluated long-period ground motions at the site of a planned long-span bridge structure in Tokyo Bay. Komori *et al.*(2005) clarified the effectiveness of strengthening the structural components of large bridges in the Metropolitan Expressway by using the simulated long-period ground motions. In addition, Abdel-Ghaffar and Nazmy (1991) revealed the three-dimensional seismic behavior of long-span cable-stayed bridges by numerical analyses. In contrast to these theoretical and numerical studies, Vilaverde and Martin (1995) carried out seismic shaking table tests on models to evaluate the effectiveness of seismic control devices for cable-stayed bridges. Kawashima *et al.*(1993) clarified the damping mechanism of cable-stayed bridges by experimental studies using 1/150-scale models. Kitazawa *et al.*(1990) clarified the effectiveness of dampers installed on the Higashi-Kobe Bridge by shaking table tests. Despite the abundance of data from these studies, the mechanisms involved in the seismic response of cable-stayed long-period bridges when subjected to a long-period component of a ground motion have not yet been sufficiently clarified from theoretical and experimental points of view. Especially, no experimental studies dealing with a long-period ground motion by considering the similarity ratios of a bridge model with a prototype cable-stayed bridge, have ever tried.

In view of the above, in this study the mechanisms associated with the seismic response of a PC cable-stayed bridge when subjected to a long-period ground motion are clarified by carrying out shaking table tests considering the similarity law. This study defines the ‘long-period’ of a ground motion as the period of more than 2.0 sec or 2.5 sec referring the definition from the field of strong motion seismology (Irikura, 2006). The natural period of the subject bridge is from 2.0 sec to 3.0 sec.

2. SHAKING TABLE TESTS

2.1. Bridge Model and Experimental Setup

The subject bridge is the Ji-Lu Bridge, which is a two-span PC cable-stayed bridge and damaged in the 1999 Chi-Chi, Taiwan earthquake (Tai and Liou, 2000). Figure 1 shows the damage to the Ji-Lu Bridge (Tasaki *et al.*, 2004). Based on the configuration of the Ji-Lu Bridge considering the necessity of the bridge model to be simplified in terms of its fabrication and construction for the tests, the similarity ratios of the model with respect to the Ji-Lu Bridge (prototype bridge) were determined as shown in Table 1 and the bridge model was designed as shown in Figure 2. The Poly-vinyl-alcohol (PVA) concrete was used as the concrete for the tower model to effectively constrain the core concrete due to the tension stress provided by fibers in the PVA concrete. The content of the PVA fibers in the concrete was 0.02 (2%) by volume. The height and the sectional area of the tower, and the sizes of the longitudinal reinforcements were determined to satisfy the similarity ratios with respect to length and flexural rigidity. The resulting sectional area of the tower was 30 mm × 30 mm, and four longitudinal reinforcements 0.9 mm in diameter with tension strengths of 336 MPa were used. Brass weights of 9.96 kg were attached at the top of the tower, as shown in Figure 2, to satisfy the similarity ratio with respect to the mass of the tower. Although the girders of the prototype bridge are formed of prestressed concrete, for the sake of ease of manufacturing, the girder of the model was steel plate of 50 mm in width and 6 mm in height to satisfy the similarity ratio with respect to the flexural rigidity. Eight brass weights of each 3.0 kg were attached to the girder to satisfy the similarity ratio with respect to the mass of the girders.

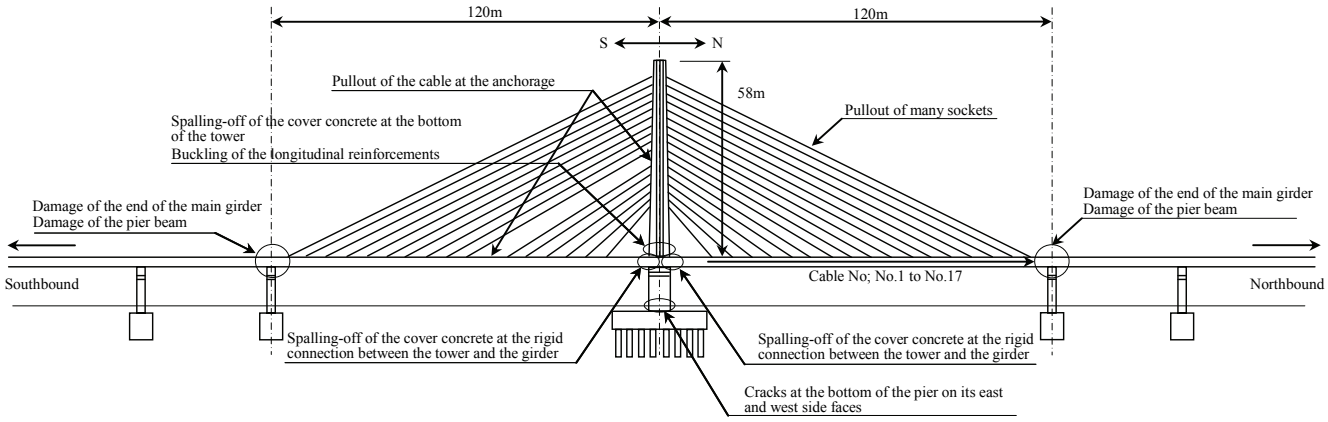

Figure 1 Damage to the Ji-Lu Bridge (Tasaki *et al.*, 2004)

Table 1 Similarity ratios

	Dimension	Similarity ratio
Acceleration	lt^{-2}	1
Length	l	100
Time	t	10
Density of mass	ρ	1
Frequency	t^{-1}	0.1
Velocity	lt^{-1}	10
Mass	ρl^3	1000000
Force	$\rho l^4 t^{-2}$	1000000
Weight	$\rho l^4 t^{-2}$	1000000
Weight per unit length	$\rho l^3 t^{-2}$	10000
Area	l^2	10000
Moment of inertia	l^4	100000000
Modulus of elasticity	$\rho l^2 t^{-2}$	100
Flexural rigidity	$\rho l^6 t^{-2}$	10000000000
Tensile rigidity	$\rho l^4 t^{-2}$	1000000
Spring coefficient in sway	$\rho l^3 t^{-2}$	10000
Spring coefficient in rocking	$\rho l^5 t^{-2}$	100000000

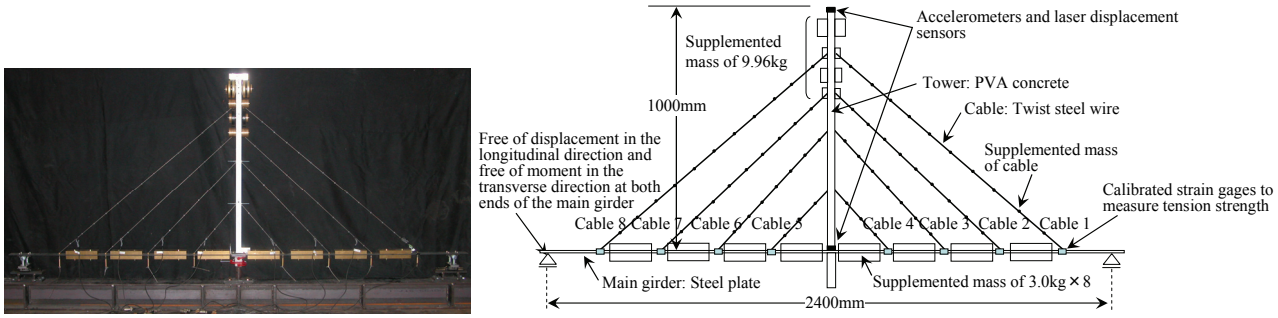

Figure 2 Bridge model

Idealized cables were designed based on the similarity ratio with respect to the force by referring to the tension strength at a permanent strain of 2%; twisted steel wires 1.5 mm in diameter with tension strength of 269.5 N at a permanent strain of 2% were used. In the prototype bridge, the 68 cables are tensioned in parallel at the center line of the girders in the longitudinal direction, thus the 34 cables should be idealized in the tests. However the number of cables was reduced from the 34 cables to the 8 ones. The reason for this is that perfectly satisfying the similarity ratios for all 34 cables is quite difficult from the viewpoint of the construction of the cable models and the stressing of their tension strength. In reducing the number of the cables, to satisfy the similarity associated with the prestressed strength of the cables between the prototype bridge and the model, and associated with the moment acting on the section of the girder with respect to the transverse axis due to the cable tension, the prestressed tension strength of each cable and its attachment positions to the girder and the tower were determined.

The pier was idealized by a rigid body made of a circular steel bar 30 mm in diameter. The free and the fixed support conditions of the longitudinal, the transverse, and the rotational movements at both ends of the girder were idealized by combining a slider and a bearing. Acceleration in the tower top and at the tower bottom in the transverse and longitudinal directions is recorded by accelerometers and displacement in the same positions as acceleration is recorded by laser displacement sensors. Tension strength of cables is measured by the strain gage attached on the edge of each cable, whose value is related with tension strength before the tests. Sampling frequency at which all data above are recorded is 1000 Hz. The average values of the dominant natural period and the damping ratio with respect to the transverse direction of the bridge model were computed based on the displacement waveforms at the top of the tower obtained from the free vibration tests. Three free vibration tests were conducted before and after each test. The computed natural periods before the tests varied from 0.311 sec to 0.325 sec and those after the tests from 0.312 sec to 0.355 sec, depending on experimental setups of the test cases. The computed damping ratios before the tests varied from 0.00594 to 0.00992. These natural periods for the bridge model correspond to a natural period of more than 3.0 sec for the prototype bridge based on the similarity ratio with respect to time. The other hand, the natural period with respect to the longitudinal direction of the bridge model was evaluated by the Fourier transforms of the acceleration waveforms obtained from the free vibration tests. The results indicate that there were several predominant coupled modes in the period ranging from 0.10 sec to 0.31 sec.

2.2. Input Ground Motions for the Shaking Table Test

Table 2 shows the test cases for the shaking table test. Uni-lateral and bi-lateral shaking table tests were conducted using the simulated ground motions at the site of the Ji-Lu Bridge simulated by Ido and Shoji (2005), and those of the anticipated Nankai earthquake at stations OSK003, OSK005, and OSK008 simulated by Kamae *et al.*(2004) The uni-lateral shaking was in the transverse direction of the bridge model, which was subjected to the EW component or the NS component of those excitations. The bi-lateral shaking was simultaneously in the transverse and longitudinal directions of the bridge model; the transverse direction was subjected to the EW component of the above excitations and the longitudinal direction was subjected to the NS component. The seismic excitations were modified based on the similarity ratios with respect to length and time. Figure 3 shows their response spectra.

Table 2 Test cases

Test No.	Direction of shaking	Input excitation	Comp.	Amplification factor of amplitude
1	TR	Simulated waveform at Ji-Lu Bridge in the 1999 Chi-Chi, Taiwan EQ.	EW	1
2		Simulated waveform at Ji-Lu Bridge in the 1999 Chi-Chi, Taiwan EQ.	EW	2
3		Simulated waveform at Ji-Lu Bridge in the 1999 Chi-Chi, Taiwan EQ.	EW	3
4		Simulated waveform at OSK008 in the anticipated Nankai EQ.	EW	1
5		Simulated waveform at OSK008 in the anticipated Nankai EQ.	EW	2
6		Simulated waveform at OSK008 in the anticipated Nankai EQ.	NS	1
7		Simulated waveform at OSK008 in the anticipated Nankai EQ.	NS	2
8		Simulated waveform at OSK008 in the anticipated Nankai EQ.	NS	3
9		Simulated waveform at OSK003 in the anticipated Nankai EQ.	EW	1
10		Simulated waveform at OSK003 in the anticipated Nankai EQ.	NS	1
11		Simulated waveform at OSK005 in the anticipated Nankai EQ.	EW	1
12		Simulated waveform at OSK005 in the anticipated Nankai EQ.	NS	1
13	TR+LG	Simulated waveform at Ji-Lu Bridge in the 1999 Chi-Chi, Taiwan EQ.	NS+EW	1
14		Simulated waveform at Ji-Lu Bridge in the 1999 Chi-Chi, Taiwan EQ.	NS+EW	2
15		Simulated waveform at OSK008 in the anticipated Nankai EQ.	NS+EW	1
16		Simulated waveform at OSK003 in the anticipated Nankai EQ.	NS+EW	1
17		Simulated waveform at OSK005 in the anticipated Nankai EQ.	NS+EW	1

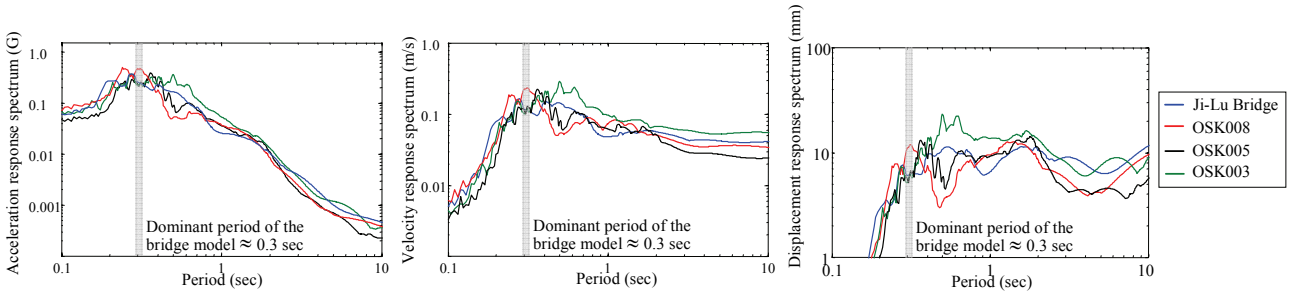

i) Acceleration response spectra ii) Velocity response spectra iii) Displacement response spectra

(a) EW component

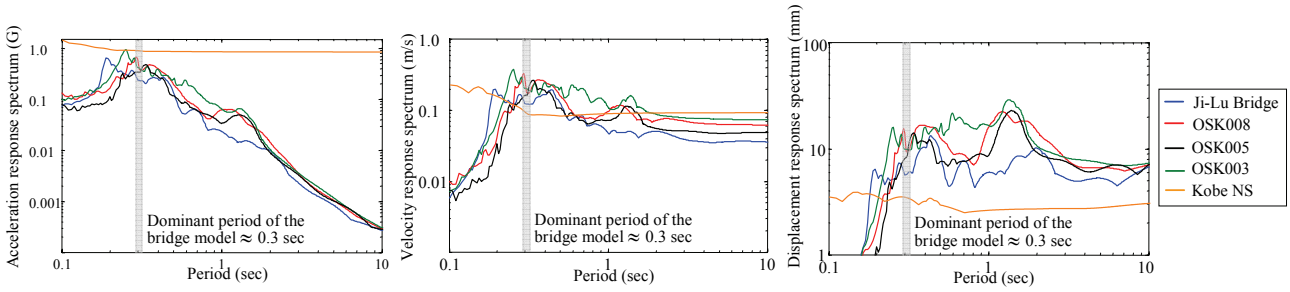

i) Acceleration response spectra ii) Velocity response spectra iii) Displacement response spectra

(b) NS component

Figure 3 Response spectra for the bridge model when subjected to input ground motion

3. SEISMIC RESPONSE SUBJECTED TO A LONG-PERIOND GROUND MOTION

3.1. Linear Seismic Response of the Bridge Model when Subjected to the Uni-Lateral Shaking

Figure 4 shows the maximum acceleration and displacement responses in the transverse direction at the top of the prototype bridge, when subjected to the simulated ground motions at the site of the Ji-Lu Bridge (Test No.1:Ji-Lu Br.EW) and those of the anticipated Nankai earthquake at stations OSK008EW, OSK003EW, and OSK005EW (Test No.4:OSK008EW, No.9:OSK003EW, and No.11:OSK005EW). Associated with all cases above, the seismic responses of the bridge model were in the linear range, where no cracks occurred in the tower. Thus, Figure 4 shows the cases where the experimental results are scaled up to those for the prototype bridge

based on the similarity ratios with respect to length and time. In addition, to compare the seismic responses of the cases subjected to the long-period excitations with those subjected to the near-field excitation (Kobe NS), Figure 4 shows the same results when subjected to the Kobe NS excitation from nonlinear seismic analysis, in which the structural modeling of the bridge model is the same as that adopted by Shoji and Kitahara (2007). In the Kobe NS case, the seismic responses of the bridge model are also in the liner range. From Figure 4, it indicates that the maximum accelerations in the cases of the Ji-Lu Br.EW, OSK003EW, OSK005EW, and OSK008EW are less than that in the Kobe NS case. In contrast, the maximum displacements in the cases of the Ji-Lu Br.EW, OSK003EW, OSK005EW, and OSK008EW are larger than that in the Kobe NS case, especially in the case of OSK008EW, where a maximum displacement of 1.35 m occurs at the top of the tower. This value corresponds to a maximum drift ratio of 1.35%, which is a large value corresponding with the response level of which seismic behavior of the tower becomes nearly equal to be nonlinear.

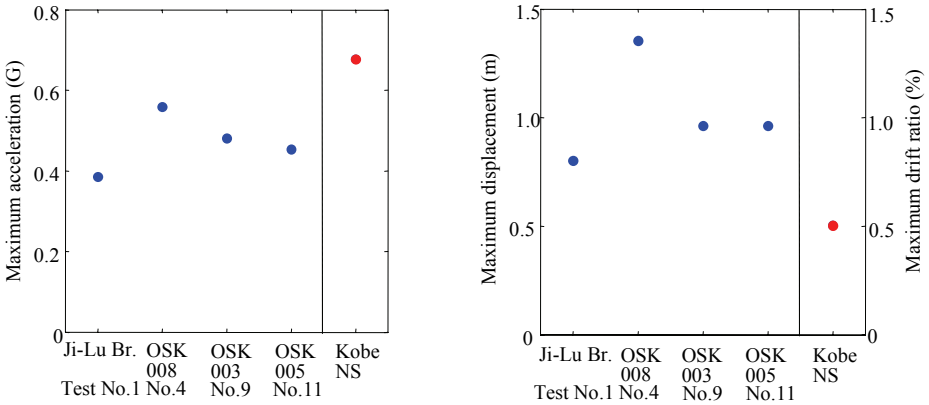

(a) Maximum acceleration response (b) Maximum displacement response

Figure 4 Maximum acceleration and maximum displacement responses in the transverse direction at the top of the tower

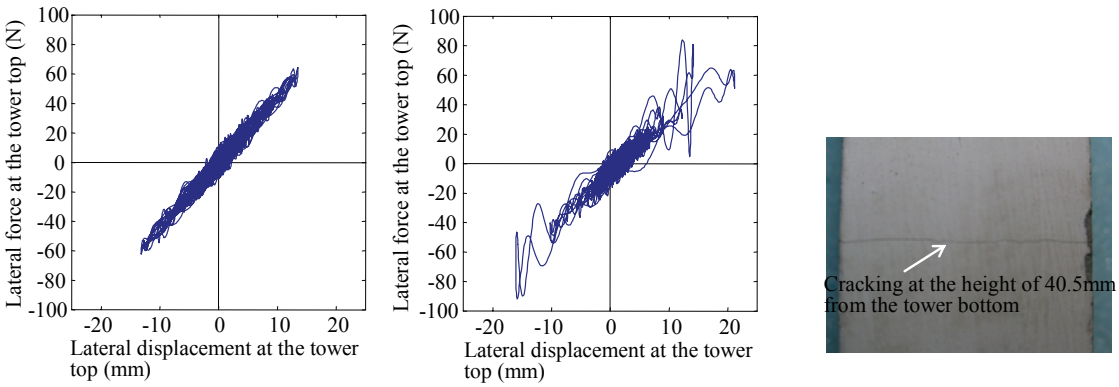

(a) In the case of the excitation equal to the OSK008 EW component (Test No.4) (b) In the case of two times the excitation of the OSK008 EW component (Test No.5)

Figure 5 Lateral force versus lateral displacement relationship at the top of the tower, depending on the amplitudes of excitations

Figure 5 shows the relationship between the lateral force and the lateral displacement at the top of the tower for uni-lateral transverse shaking in the case of the OSK008EW (Test No.4) and two times the excitation of the OSK008 EW component (Test No.5:2 times-OSK008EW). The former case shows a linear response of the tower, previously shown in Figure 4, whereas the latter one shows a nonlinear response that causes cracks in the tower. Thus, although the relationship between the lateral force and the lateral displacement in the case of OSK008EW is limited in the linear range (Figure 5(a)), its response level reaches almost same one to be nonlinear hysteretic behavior that the case of 2 times-OSK008EW shows (Figure 5(b)). The occurrence of larger displacement at the tower top in the case of the long-period excitations than that in the case of the Kobe NS excitation, results from the larger displacement response at the tower top in the transverse direction on the 1st mode of the bridge model,

due to the matching of the dominant natural period of the bridge model and that of the long-period excitations, shown in Figure 3. Therefore, even though the acceleration response of the long-period bridge does not become larger, the displacement response could become larger when subjected to the long-period ground motions, and it is likely that this mechanism causes the nonlinear hysteretic behavior of the tower shown in Figure 5(b).

3.2. Residual Displacement at the Top of the Tower

Figure 6 shows the displacement responses at the top of the tower for uni-lateral transverse shaking equal to three times the excitation of the simulated ground motion at the Ji-Lu Bridge (Test No.3:3 times-Ji-Lu Br.EW), 2 times-OSK008EW (Test No.5), and two times the excitation of the OSK008 NS component (Test No.7:2 times-OSK008NS). In all cases, a crack occurred in the tower model; the values of the responses resulting from the tests are not scaled up to in Figure 6. From Figure 6, although the maximum displacements at the top of the tower for different ground motions were nearly the same, namely, about 20 mm, the maximum residual displacements at the top of the tower were quite different depending on the excitations applied. Whereas a slight residual displacement of 0.014% per unit of drift occurred in the case of 3 times-Ji-Lu Br.EW (Test No.3), larger residual displacements of 0.29% and 0.12% per unit of drift occurred for the cases of 2 times-OSK008EW (Test No.5) and 2 times-OSK008NS (Test No.7), respectively.

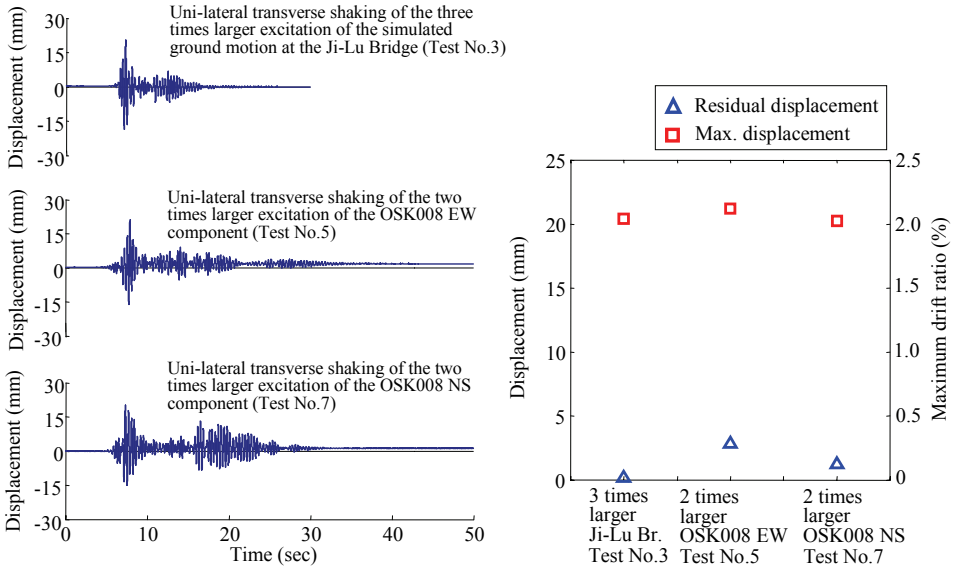

(a) Displacement at the top of the tower in the transverse direction

(b) Comparison of residual displacement with maximum displacement at the tower top

Figure 6 Residual displacement, depending on the duration of the excitations

For the three cases, the relationship between the lateral force and the lateral displacement was computed for four different stages in the response time series, as shown in Figure 7: when the maximum displacement occurred when the main large excitation subjected (stage 1), immediately after stage 1 (stage 2), when the displacement response decreased after stage 2 (stage 3), and when the displacement response increased after stage 3 due to the subsequent large excitation (stage 4). The residual displacement at the top of the tower did not occur in stage 1 or stage 2 for the case of 3 times-Ji-Lu Br.EW (Test No.3), whereas those occurred in stage 2 for the cases of 2 times-OSK008EW (Test No.5) and 2 times-OSK008NS (Test No.7), and these residual displacements became continuous with those at the end of the displacement waveforms. Focusing on the increase of the residual displacement after stage 2, in both cases of 2 times-OSK008EW (Test No.5) and 2 times-OSK008NS (Test No.7) the large displacement response in stage 4 after 15 sec caused a slight increase in the residual displacement at the top of the tower. The results indicate that the subsequent large excitation after the maximum displacement had no effect on whether the residual displacement at the tower top occurred or not, whereas it had a slight effect on the degree of increasing the residual displacement at the tower top.

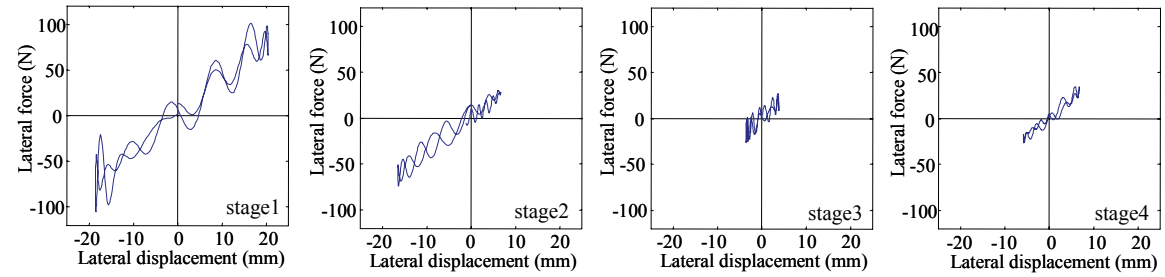

(a) Uni-lateral transverse shaking equal to three times the excitation of the simulated ground motion at the Ji-Lu Bridge (Test No.3)

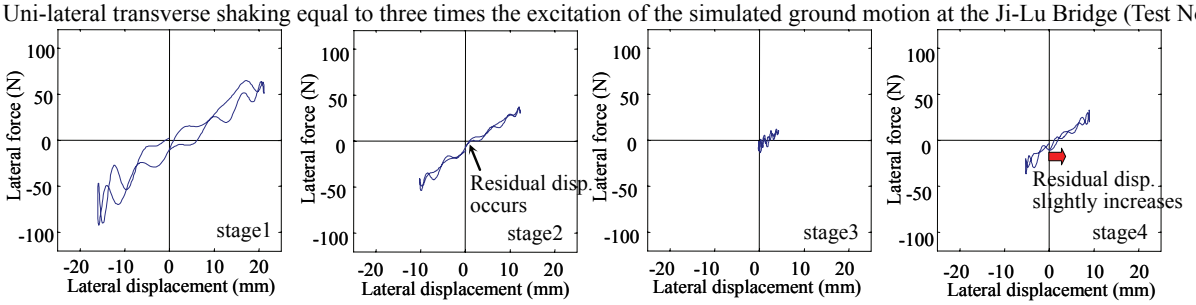

(b) Uni-lateral transverse shaking equal to two times the excitation of the OSK008 EW component (Test No.5)

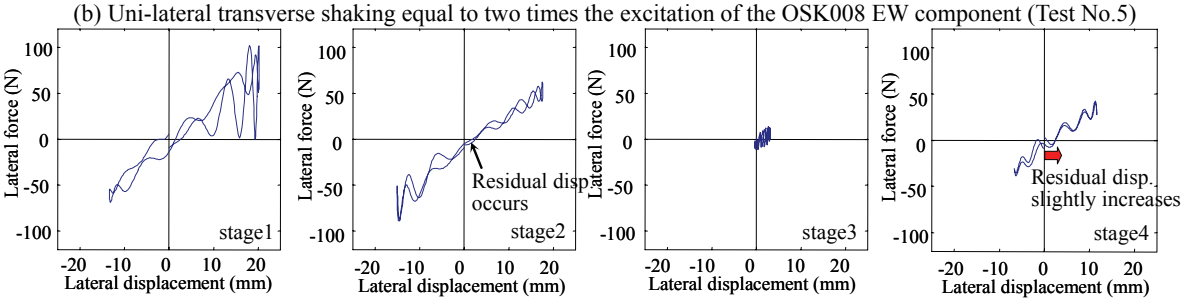

(c) Uni-lateral transverse shaking equal to two times the excitation of the OSK008 NS component (Test No.7)

Figure 7 Lateral force versus lateral displacement relationship for four different stages in the time series

4. CONCLUSIONS

In this study the mechanisms associated with the seismic response of a PC cable-stayed bridge when subjected to a long-period ground motion were clarified based on shaking table tests considering the similarity law. The simulated long-period ground motions in the 1999 Chi-Chi, Taiwan earthquake and the anticipated Nankai earthquake were used as the input ground motions in the shaking table tests. The following conclusions were obtained from the study:

1) Larger maximum displacements were found at the tower top for the long-period excitations compared with that obtained from the seismic response analysis using the JMA Kobe record (near-field excitation). This resulted from larger displacement response at the tower top in the transverse direction depending on the 1st mode of the bridge model, due to the matching of the dominant natural period of the bridge model and that of the long-period ground motions. Thus, even though the acceleration response of the long-period bridge is not amplified, the displacement response could become larger when subjected to the long-period ground motions, and it is likely that this mechanism may cause the nonlinear hysteretic behavior of the tower.

2) The subsequent large excitation after the maximum displacement at the tower top did not affect the occurrence of the residual displacement of the tower, whereas it slightly affected the degree of increasing the residual displacement. The occurrence of the residual displacement on structural components for the long-period bridge causes the difficulty in the repair process once the bridge is damaged, therefore we must pay more attention to the increasing of the residual displacement at the tower subjected to the subsequent large excitation that a long-period ground motion contains.

ACKNOWLEDGEMENTS

This research was sponsored by the National Research Institute for Earth Science and Disaster Prevention (NIED) under the 2005 grant provided for seismic experimental research on bridges titled 'International Joint Model Research for the Application of the Full-Size Three-Dimensional Vibration Destruction Facility (E-Defense)'. The authors specially thank Professor K. Kamae and Dr. H. Kawabe at Research Reactor Institute, Kyoto University, for providing the simulated waveforms of the anticipated Nankai earthquake. Moreover the authors deeply appreciate the valuable assistance and support from Professor T. Kanakubo, Dr. K. Shimizu, Professor Y. Sakai and Mr. A. Kojima at Graduate School of Systems and Information Engineering, University of Tsukuba, regarding the design and the manufacturing for tower models used for the tests, and carrying out a series of the shaking table tests. We are much grateful to Dr. A. Numata, Mr. T. Ikeda, Mr. K. Taguchi and the other members of Disaster Prevention R&D Research Institute, Tobishima Corporation, for the use of the experimental facility, the valuable assistance and support of our study.

REFERENCES

Abdel-Ghaffar, A. M. and Nazmy, A. S. (1991). 3-D nonlinear seismic behavior of cable-stayed bridges. *Journal of Structural Engineering* **117:11**, ASCE, 3456-3476.

Ido, Y. and Shoji, G. (2005). Evaluation of input ground motions at the site of the Ji-Lu Bridge in the 1999 Chi-Chi, Taiwan earthquake. *Proceedings of the 8th Symposium on Ductility Design Method for Bridges*, JSCE, 441-446 (in Japanese).

Irikura, K. (2006). Long-period ground motions from devastating great earthquakes and action plans for earthquake disaster mitigation. *Chikyu Monthly* **55**, 6-16 (in Japanese).

Kamae, K., Kawabe, H. and Irikura, K. (2004). Strong ground motion prediction for huge subduction earthquakes using a characterized source model and several simulation techniques. 13th World Conference on Earthquake Engineering, Vancouver, B.C., Canada, Paper No. 655 (CD-ROM).

Kawashima, K., Unjoh, S., and Tunomoto, M. (1993). Estimation of damping ratio of cable-stayed bridges for seismic design. *Journal of Structural Engineering* **119:4**, ASCE, 1015-1031.

Kitazawa, M., Ishizaki, H., Emi, S. and Nishimori, K. (1990). Characteristics of earthquake responses and aseismic design on the long-period cable-stayed bridge (Higashi-Kobe Bridge) with all free movable shoes in longitudinal direction. *Journal of Structural and Earthquake Engineering* **422:I-14**, JSCE, 343-352 (in Japanese).

Komori, K., Kikkawa, H., Odagiri, N., Kinoshita, T., Mizoguchi, T., Fujino, Y. and Yabe, M. (2005). Basic principles and design ground motions in seismic retrofit design of large cable-supported bridges on the Tokyo Metropolitan Expressway. *Journal of Structural and Earthquake Engineering* **794:I-72**, JSCE, 1-19 (in Japanese).

Otsuka, H., Somerville, P.G. and Sato, T. (1998). Estimation of broadband strong ground motions considering uncertainty of fault parameters. *Journal of Structural and Earthquake Engineering* **584:I-42**, JSCE, 185-200 (in Japanese).

Shoji, G. and Kitahara, J. (2007). Seismic response of a PC cable-stayed bridge subjected to a long-period seismic excitation. *Proceedings of the 4th Korea-Japan Workshop on New Direction for Enhancement of Structural Performance*, Hamamatsu, Japan, 37-44.

Tai, J.C., and Liou, Y.Y. (2000). Retrofit on Ji-Lu Cable Stayed Bridge after 921 Chi-Chi earthquake. *Proceedings of the 2nd International Workshop on Mitigation of Seismic Effects on Transportation Structures*, National Center for Research on Earthquake Engineering, Taipei, Taiwan, R.O.C., 65-79.

Tasaki, K., Kosa, K., Ikeda, T. and Ogo, M. (2004). Detailed investigation of PC cable-stayed bridge (Ji-Ji-Da Bridge) damaged to the Taiwan Chi-Chi earthquake. *Journal of Structural Engineering* **50A**, JSCE, 487-494 (in Japanese).

Vilaverde, R. and Martin, S. C. (1995). Passive seismic control of cable-stayed bridges with damped resonant appendages. *Earthquake Engineering and Structural Dynamics* **24**, 233-246.